HAL
open science

# Specific salt effects on thermophoresis of charged colloids

Kyriakos A. Eslahian, Arghya Majee, Michael Maskos, Alois Würger

## To cite this version:

Kyriakos A. Eslahian, Arghya Majee, Michael Maskos, Alois Würger. Specific salt effects on thermophoresis of charged colloids. Soft Matter, 2014, 10, pp.1931-1936. 10.1039/C3SM52779D . hal-00952801

**HAL Id: hal-00952801**

**https://hal.science/hal-00952801**

Submitted on 27 Feb 2014

**HAL** is a multi-disciplinary open access archive for the deposit and dissemination of scientific research documents, whether they are published or not. The documents may come from teaching and research institutions in France or abroad, or from public or private research centers.

L'archive ouverte pluridisciplinaire **HAL**, est destinée au dépôt et à la diffusion de documents scientifiques de niveau recherche, publiés ou non, émanant des établissements d'enseignement et de recherche français ou étrangers, des laboratoires publics ou privés.

Distributed under a Creative Commons Attribution - ShareAlike 4.0 International License

# Specific Salt Effects on Thermophoresis of Charged Colloids

Kyriakos A. Eslahian[1,2], Arghya Majee[3,4,5], Michael Maskos[2], Alois Würger[5]
[1] *Bundesanstalt für Materialforschung und Prüfung, Unter den Eichen 87, 12205 Berlin, Germany*
[2] *Institut für Mikrotechnik Mainz GmbH, Carl-Zeiss-Strasse 18-20, 55129 Mainz, Germany*
[3] *Max-Planck-Institut für Intelligente Systeme, Heisenbergstrasse 3, 70569 Stuttgart, Germany*
[4] *Institut für Theoretische Physik IV, Universität Stuttgart, Pfaffenwaldring 57, 70569 Stuttgart, Germany and*
[5] *Laboratoire Ondes et Matière d'Aquitaine, Université de Bordeaux & CNRS, 351 cours de la Libération 33405 Talence, France*

We study the Soret effect of charged polystyrene particles as a function of temperature and electrolyte composition. As a main result we find that the Soret coefficient is determined by charge effects, and that non-ionic contributions are small. In view of the well-kown electric-double layer interactions, our thermal field-flow fractionation data lead us to the conclusion that the Soret effect originates to a large extent from diffusiophoresis in the salt gradient and from the electrolyte Seebeck effect, both of which show strong specific-ion effects. Moreover, we find that thermophoresis of polystyrene beads is fundamentally different from proteins and aqueous polymer solutions, which show a strong non-ionic contribution.

PACS numbers:

## I. INTRODUCTION

When applying a temperature gradient to a colloidal suspension, molecules and nanoparticles migrate to the cold or to the hot, depending on the solute and solvent properties [1–4]. In recent years, this Soret effect, or thermophoresis, has been used for colloidal confinement to a micron-sized hot spot in a channel or thin film [5–7], and for self-propulsion of hot Janus particles in active colloids [8–10]. The underlying thermal forces are very sensitive to the electrolyte composition. Thus colloids move to the cold side in NaCl solution and to the hot in NaOH, because of the Seebeck effect which takes opposite signs in these electrolytes [11–14]. The related electric field has been discussed in view of translocating DNA through nanopores [15] and accumulating charge in a micron-size hot spot [16, 17]. More generally, thermophoresis shows specific-ion effects [18, 19] similar to the Hofmeister series of protein interactions. As another signature for charge effects, the electrostatic repulsion of nearby particles gives rise to a characteristic dependence on volume-fraction and salinity [20, 21]

The temperature dependence of thermophoresis is poorly understood, in particular the strong increase with $T$ and the change of sign that occur in many instances [22–26]. In a study on lysozyme protein, Iacopini *et al.* separated the effect of temperature and salinity [22]; their data give clear evidence for an important non-ionic interaction that dominates the temperature dependence. This has been confirmed for non-ionic surfactants [26, 27] and PNIPAM microgels [24, 25]. A phenomenological law proposed by Piazza describes remarkably well the behavior of non-ionic solutes, proteins, polyelectrolytes, and charged latex beads [26]. Regarding the latter, there is so far no direct proof for a non-ionic driving mechanism. To know whether it exists or not, is important for an efficient surface functionalization of self-propelling colloids.

The present paper addresses two questions on thermophoresis of charged particles: First, is there a non-ionic contribution and, second, what is the origin of the temperature dependence? We report on thermal field-flow fractionation (ThFFF) measurements of the Soret coefficient of polystyrene sulfonate (PS) beads as a function of electrolyte composition and temperature. In view of the theory of phoretic motion of colloids, our data strongly suggest that the answer to the above questions is intimately related to the temperature-induced salt-ion gradients.

The paper is organized in the following way. Sect. 2 gives details of our experimental setup, and Sect. 3 an overview of the theoretical description of thermophoresis due to electric-double layer forces. The effects of the electrolyte composition and temperature are discussed in Sects. 4 and 5. We conclude in Sect. 6 with a discussion of our main results and a comparison to protein thermophoresis.

## II. EXPERIMENTAL SECTION

We briefly present the principle of ThFFF as shown in Fig. 1. The colloidal suspension is injected at the channel entrance and, after an equilibration time of one minute [28], reaches a steady state with vertical concentration profile $c = c_0 e^{-z/\ell}$, where the retention length $1/\ell = S_T \Delta T/w$ depends on the Soret coefficient $S_T$, the temperature difference $\Delta T = T_h - T_c$ across the channel, and its width $w$. In our setup the channel length is 46.4 cm, the breadth 1.8 cm, and the width $w$ =100 $\mu$m. Pumping the suspension through the channel results in a parabolic velocity profile. At the exit, the colloidal content is determined by detection of the UV-absorption as a function of time. Typical elution profiles as in Fig. 1c, consist of a strong Gaussian feature at

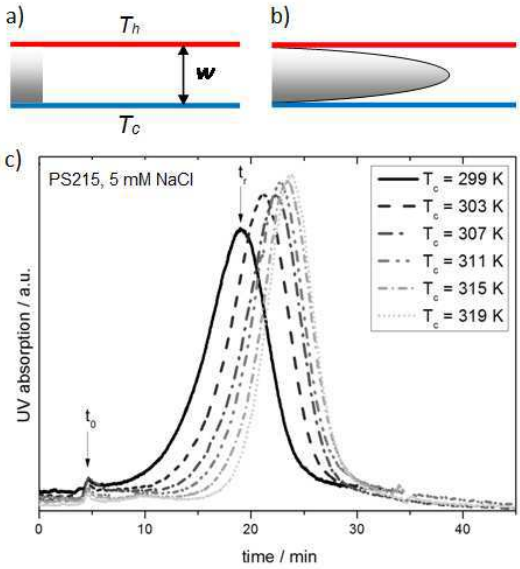


FIG. 1: Schematic view of our ThFFF setup. a) The Soret equilibrium state in the vertical temperature difference is prepared at the entrance of the channel, with a vertical concentration profile $c = c_0 e^{-z/\ell}$. b) Pumping the suspension through the channel results in a parabolic velocity profile. At the exit, the colloidal content is determined by detection of the UV-absorption as a function of time. c) Typical elution profiles consist of a strong Gaussian feature at $t = t_r$ that describes the arrival of the particles accumulated close to the lower wall. We show elution patterns at different temperatures. At higher $T$, the position of the Gaussian is shifted to later times, implying a smaller retention length $\ell$ and thus a higher Soret coefficient.

$t = t_r$ that describes the arrival of the particles accumulated close to the upper or lower wall; the small precursor peak occurs at the moment where the front of the parabolic flow profile reaches the exit. At higher $T$, the position of the Gaussian is shifted to later times, implying a smaller retention length $\ell$ and thus a higher Soret coefficient. In all experiments the flow rate is 0.3 mL/min and the colloidal mass fraction at the moment of injection is in the order of $10^{-4}$; the temperature difference is in the range $\Delta T = 15...25$ K for the data shown in Fig. 2 and 3, and $\Delta T = 10...15$ K for those in Figs. 4 and 5. The effective temperature is calculated by assuming a linear temperature profile through the channel and taking the concentration-weighted mean value. For positive and negative $S_T$ this gives $T = T_c + \Delta T(\ell/w)$, and $T = T_h - \Delta T(\ell/w)$, respectively.

The Soret coefficient is determined following a standard procedure [28]. The channel void time $t_0$, which is given by the centre of gravity of the elugram of one non-retained sample, is divided by the retention time to calculate the retention ratio $R = t_0/t_r$. The almost parabolic velocity profile results in a characteristic elution pattern that allows us to determine the length $\ell$ through the relation $R = 6\lambda \coth(1/2\lambda) - 12\lambda^2$, where $\lambda = \ell/w = 1/S_T \Delta T$ [29]. For most of our data, $\lambda$ is in the range from 2 to 6%. In the calculated retention parameters, we account for deviations of the flow profile due to the temperature dependent viscosity. Retention parameters have to be corrected in terms of the deviation parameter [30], taking the not ideal flow profile into account, which results from the temperature dependence of the solvent [31]. ThFFF does not distinguish whether the colloid accumulates at the upper or lower plate, and thus provides only the absolute value $|S_T|$ of Soret coefficient. Thus the sign has to be inferred from continuity of the data and from previous experiments.

The samples PS 90 and PS 136 are prepared by surfactant-free emulsion polymerization, according to Juang and Krieger [32]. Two-phase polymerization is performed in a glass reactor, thus ensuring optimized stirring and temperature control. After heating the reactor up to 65°C, 177.7 g of water and 56.8 g of styrene are added. The difference between preparation of PS 90 and PS 136 is the amount of ionic stabilizing comonomer introduced: 0.63 g (PS 90) and 0.41 g (PS 136) of 4-styrene sulfonate. After 5 min of homogenization, the radical initiator potassium persulfate, 0.36 g solved in 10 g of water, is added drop-wise. The reaction is kept alive for 24 h, and then latex emulsions are cooled down to room temperature, filtered and dialyzed. The stability of resulting colloidal suspensions is given by electrostatic repulsion, caused exclusively by the introduced sulfonate groups. The sample PS 215 is purchased from Thermo Fisher Scientific (Waltham, MA, USA), and used without further treatment.

All experiments are performed in de-ionized water ($18.2 \times 10^4 \Omega$m) without adding surfactant. Except styrene which has to be distilled in prior to the synthesis, all chemicals are introduced as purchased in analytical grade from Merck (Darmstadt, Germany). Hydrodynamic radii of the particles used in this report are determined by dynamic multi-angle light scattering and the spherical shape is verified by transmission electron microscopy. All samples reveal having a very low polydispersity index.

## III. CHARGE-DRIVEN THERMOPHORESIS

Charge effects on colloidal motion in a non-uniform electrolyte solution arise from the interaction with the non-uniform electric double-layer [34]. In our systems the Debye screening length $\kappa^{-1}$ is small as compared to the particle size, and the surface potential $\zeta$ takes moderate values. Thus viscous effects can be treated in boundary layer approximation, and the screened electrostatics can be evaluated to second order in $\zeta$. Then the particle velocity reads [4]

$$u = -\frac{\varepsilon\zeta^2}{12\eta}\left(\frac{\nabla T}{T} - \frac{\nabla n_0}{n_0} - \frac{\nabla\varepsilon}{\varepsilon}\right) + \frac{\varepsilon\zeta}{\eta}E, \qquad (1)$$

with the solvent viscosity $\eta$, permittivity $\varepsilon$, and salinity $n_0$, and an applied electric field $E$. The terms in parentheses describe motion in a temperature gradient [35], in a salt gradient [36], and due to an electrostrictive force [37]; the particle moves toward lower temperature but higher salinity and permittivity. The last term in (1) accounts for electrophoresis in an electric field $E$, with the Helmholtz-Smoluchowksi mobility $\varepsilon\zeta/\eta$.

Here we deal with an applied thermal gradient and its companion fields induced by the temperature dependent properties of the electrolyte solution according to

$$\tau = -\frac{T}{\varepsilon}\frac{d\varepsilon}{dT}, \quad \alpha = -\frac{T}{n_0}\frac{dn_0}{dT}, \quad E = S\nabla T. \tag{2}$$

Parameter $\tau$ accounts for the temperature-dependent permittivity of water. The solvation enthalpies of positive and negative salt ions vary with temperature; they result in a non-uniform salinity with thermal diffusion factor $\alpha$ and a thermoelectric field with Seebeck coefficient $S$. With the quantities defined in (2) the particle velocity reads $u = -D_T\nabla T$, where the companion fields are absorbed in the mobility $D_T$. Its ratio with the Stokes-Einstein coefficient $D = k_BT/6\pi\eta a$ gives the Soret coefficient $S_T = D_T/D$, which varies linearly with the particle radius $a$. From the above equations we have

$$S_T = \frac{6\pi a}{k_BT^2}\left(\frac{\varepsilon\zeta^2}{12}(1+\tau+\alpha) - \varepsilon\zeta ST\right), \tag{3}$$

where the expressions in parentheses have the dimension of a force, and take typical values of a few pN. A positive sign of $S_T$ means that the particle moves to lower temperatures.

It is instructive to compare the magnitude of the different contributions to $S_T$. With $a = 215$ nm in the overall prefactor and $\zeta = -50$ mV, we find that Ruckenstein's thermo-osmotic term, that is, the "1" in Eq. (3) contributes 0.1 $\mathrm{K}^{-1}$, and the electrostrictive force $\propto \tau$ about 0.2 $\mathrm{K}^{-1}$. In NaCl solution, the specific-ion effects with coefficients $\alpha$ and $S$ contribute 0.4 and 0.6 $\mathrm{K}^{-1}$, respectively; in other words, the four terms are positive and of the same order of magnitude. In NaOH solution, however, the ion-specific effects contribute 0.6 and $-3.5$ $\mathrm{K}^{-1}$. These numbers imply that the Soret effect is to a large extent determined by the Seebeck and diffusiophoresis contributions. For negatively charged particles in NaOH solution, one expects the Seebeck term to result in a negative Soret coefficient [12].

Colloidal particles dispersed in an electrolyte solution constitute a quaternary system. An effective binary system as in Eq. (3) is obtained by eliminating the salt ion concentrations $n_\pm$ as variables; thus the $\zeta$-potential accounts for well-known composition of the electric-double layer. The parameters $\alpha$ and $S$ depend on the non-uniform salinity and the surface charges related to the Seebeck thermopotential. This reduction is achieved by solving the diffusion equation for thermally driven ion currents and by replacing $\nabla n_\pm$ with their stationary values [4, 38]. This relies in particular on the fact that the salt relaxation times are much shorter than that of the colloidal distribution function. Moreover, at sufficiently small colloidal volume fractions, the back-reaction of the colloidal macro-ions on $\alpha$ and $S$ can be neglected [14].

## IV. ELECTROLYTE COMPOSITION

### A. Specific-ion effects

Fig. 2 shows the Soret coefficient of 215 nm PS beads in a 1 mM solution of $\mathrm{NaCl}_{1-x}\mathrm{OH}_x$ as a function of the composition parameter $x$. The data show a linear variation with $x$; those at 41° C change of sign at $x \approx \frac{1}{2}$. These findings are in agreement with previous studies reporting $S_T > 0$ in NaCl and $S_T < 0$ in NaOH [11, 13]; a similar linear dependence on composition was reported for SDS micelles in a mixed electrolyte [13]. Moreover, the data at 26° and 41° C indicate that the Soret coefficient in NaCl solution increases with temperature.

The only ion-specific quantities in Eq. (3) are the Seebeck coefficient $S$ and the thermal diffusion factor $\alpha$; for a mixed electrolyte we write these quantities as mole-fraction weighted averages,

$$\begin{aligned} S &= (1-x)S_{\mathrm{NaCl}} + xS_{\mathrm{NaOH}}, \\ \alpha &= (1-x)\alpha_{\mathrm{NaCl}} + x\alpha_{\mathrm{NaOH}}. \end{aligned} \tag{4}$$

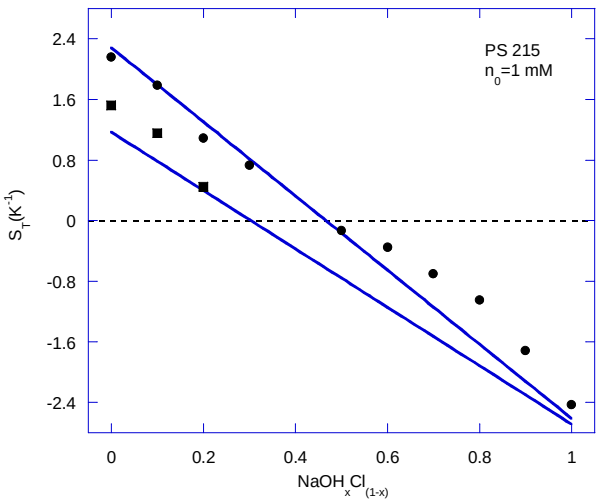


FIG. 2: Soret coefficient of 215 nm PS beads in a mixed electrolyte $\mathrm{NaCl}_{1-x}\mathrm{OH}_x$. The data at 41° C (circles) show a linear dependence on $x$, and a change of sign at $x \approx \frac{1}{2}$; those at 26° C (squares) indicate that in NaCl solution, $S_T$ strongly increases with temperature. The solid lines are calculated from Eq. (3) with $\zeta = -38$ mV, $\varepsilon = 78\varepsilon_0$, and $\tau = 1.4$; the fit values for the Seebeck coefficient $S$ and thermal diffusion factor $\alpha$ compare favorably with those measured at room temperature by Agar [39]. As discussed below, the temperature dependence of $S$ and $\alpha$ agrees with Eq. (5).

from the numbers given in Table I it is clear that $\alpha$ increases with $x$, whereas the Seebeck coefficient strongly decreases and changes sign. Moreover, with typical values of the surface potential of less than mV, one finds that the composition dependence of Eq. (3) is dominated by the Seebeck term. Since most colloids carry a negative surface charge, one expects quite generally a negative Soret coefficient in NaOH solution.

The fit curves are calculated with constant $\zeta$-potential and the salt parameters given in Table I. We have neglected various additional dependencies, such as the well known variation of the $\zeta$-potential with the pH value. Indeed, our measurements (Stabino) show that, depeding on salinity, $\zeta$ varies by about 10 to 30 percent upon replacing NaCl with NaOH. Including this dependence in the fits would merely modify the parameters $S$ and $\alpha$, but not affect our conclusions.

### B. Salinity

In Fig. 3 we plot the Soret coefficient in NaCl solution as a function of the salinity $n_0$. First $S_T$ increases with $n_0$, attains a maximum at about 5 mM, and then drops to small values beyond the resolution of our experiment. The behavior between 10 and 100 mM arises from the variation of the surface potential with salinity in the framework of Debye-Hückel approximation, $\zeta \propto n_0^{-1/2}$. This law ceases to be valid at lower salinity, as is well-known from electrophoresis [42].

As a possible mechanisms for the dependence at low electrolyte strength, and in particular for the occurrence of a maximum, we mention the surface conductivity contribution, similar to well-known reduction of the electrophoretic mobility [42]. On the other hand, there are several effects specific for thermophoresis that have hardly been investigated so far, such as the collective thermoelectric effect [14], or the fact that the coefficients $S$ and $\alpha$ depend significantly on salinity [40].

In moderate or weak electrolytes, there is no satisfactory model for the surface potential and its subtle dependencies on pH, temperature, and salinity. In order to account for the variation of $S_T$ with salinity, we take in all fits $\zeta = -38$ mV at 1 mM, $\zeta = -53$ mV at 5 mM, and $\zeta = -6.5$ mV at 100 mM. The value at 5 mM agrees with the measured $\zeta$-potential over the temperature range studied here; those at 1 and 100 mM are in accord with Fig. 3 and more generally with electrophoretic mobility data.

TABLE I: Seebeck coefficient $S$ and thermal diffusion factor $\alpha$ of dilute solutions of NaCl and NaOH. The experimental values are determined from the heats of transport $Q^*_{\rm Na}$ =3.5 kJ/mole, $Q^*_{\rm Cl}$ =0.5 kJ/mole, $Q^*_{\rm OH}$ =17.2 kJ/mole, measured by Agar [39], according to $\alpha_{\rm NaA} = (Q^*_{\rm Na} + Q^*_{\rm A})/2k_BT$ and $S_{\rm NaA} = (k_B/e)(Q^*_{\rm Na} - Q^*_{\rm A})/2k_BT$. The fit values are used for the theory curves in Fig. 2. These values agree with the linear temperature dependence for NaCl solutions given in Eq. (5).

| | $\alpha_{\rm NaCl}$ | $\alpha_{\rm NaOH}$ | $S_{\rm NaCl}$ ($\mu$V/K) | $S_{\rm NaOH}$ ($\mu$V/K) |
|---|---|---|---|---|
| exp 25° C | 0.8 | 4.1 | 52 | −238 |
| fit 26° C | 1.2 | 4.8 | 56 | −296 |
| fit 41° C | 2.9 | 4.8 | 138 | −296 |

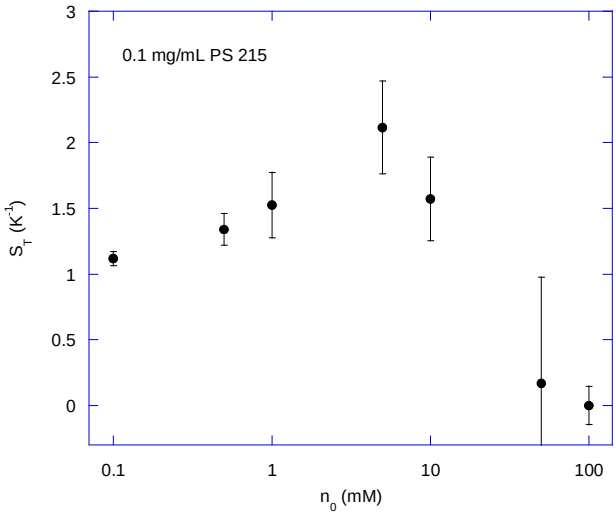


FIG. 3: Soret coefficient of 215 nm PS beads in NaCl solution as a function of the electrolyte strength at $T_C = 299$K with $\Delta T = 15$ K. For high salinity, $n_0 > 10$ mM, inserting the Debye-Hückel law $\zeta \propto n_0^{-1/2}$ in (3) gives $S_T \propto n_0^{-1/2}$ and $\propto n_0^{-1}$ for the Seebeck term and the remainder, respectively; this agrees at least qualitatively with the data. Yet these laws cease to be valid at lower salinity; our data, and in particular the occurrence of a maximum, are similar to the well-known behavior of the electrophoretic mobility, which is to large extent determined by the salinity dependence of the $\zeta$-potential [42].

## V. TEMPERATURE DEPENDENCE

Soret data for various colloids show a strong and surprisingly universal temperature dependence [22–27]. Here we present data for both NaCl and NaOH solutions that are essential for the main results of this paper.

### A. NaCl solution

According to Fig. 3, the Soret coefficient of polystyrene particles vanishes at high salinity. In order to determine whether this is the case at all temperatures, we plot in Fig. 4 Soret data measured at different electrolyte strength as a function of $T$. The main features are a roughly linear variation with temperature, a strong reduction upon increasing the electrolyte strength, and a

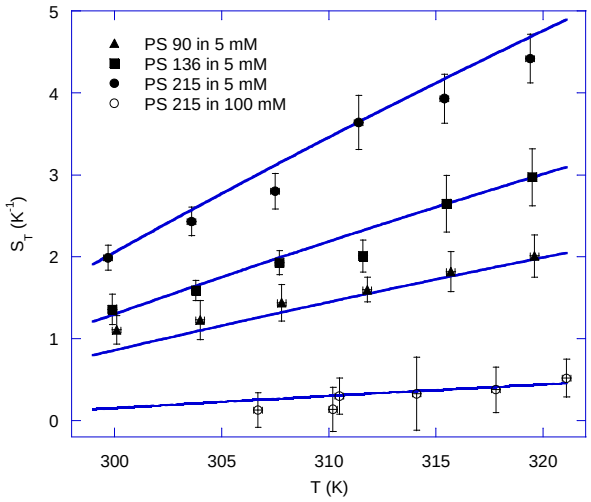


FIG. 4: Soret coefficient in NaCl solution as a function of temperature. The solid lines are calculated from (3) with $\zeta = -53$ mV at 5 mM and $-6.5$ mV at 100 mM; we assume a linear variation of $S$ and $\alpha$ according to Eq. (5), with values at 25° C from Table I.

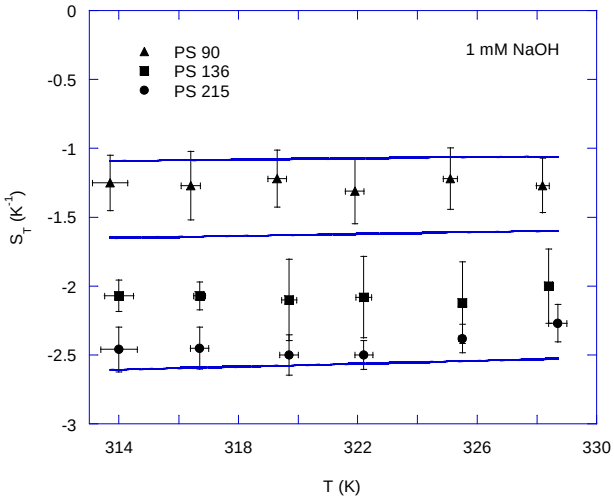


FIG. 5: Soret coefficient of PS beads in NaOH solution. The electrolyte thermal diffusion Seebeck coefficients $\alpha$ and $S$ are kept constant; the slight temperature dependence arises from the prefactor in (3).

linear increase with the particle size. These findings lead us to two main conclusions of the present work.

*First,* the Soret effect of 215 nm beads in 5 mM NaCl is almost ten times stronger than in 100 mM solution, and this over the range from 25° C to 50° C. This uniform reduction provides strong evidence that thermophoresis of polystryene beads arises from charge effects only. They exclude the existence of a significant non-ionic contribution to $S_T$; the values in 100 mM solution may be taken as an upper bound. In contrast to our results, the Soret effect of proteins arises essentially from a non-ionic mechanism, as shown by a study on lysozyme at variable eletrolyte strength and temperature [22]. This implies that thermophoresis of PS beads differs fundamentally from that of proteins.

*Second,* the Soret coefficient at 46° C is about twice as large as at 26° C. Since the overall prefactor in (3), and the parameters $\zeta$, $\varepsilon$, and $\tau$, hardly vary with temperature, we conclude that the $T$-dependence of $S_T$ is necessarily related to the Seebeck coefficient $S$ and the thermal diffusion factor $\alpha$ of the salt solution. Moreover, the data confirm the well-known fact that the Soret coefficient is proportional to the particle size [4, 33]. The temperature dependence qualtitatively agrees with previous studies on PS beads [23, 26].

In order to make the above arguments more quantitative, we have fitted the temperature dependence in terms of a minimal model for the Seebeck coefficient and the thermal diffusion factor,

$$S_{\rm NaCl} = S^0_{\rm NaCl}\,(1+\xi t)\,, \quad \alpha_{\rm NaCl} = \alpha^0_{\rm NaCl}\,(1+\xi t)\,, \quad (5)$$

where $t = T - 298$K and the superscript "0" indicates room-temperature values according to Table I. The straight lines in Fig. 4 are calculated from Eq. (3) with the slope parameter $\xi = 0.14$ K$^{-1}$. There seem to be no data on the $T$-dependence of the Seebeck coefficient. The slope measured for the thermal diffusion coefficient $\alpha$ of very strong electrolytes of about 1 M, is about four times smaller [40]; at low salinity a stronger but non-linear increase of $\alpha$ was observed [41]. These experimental findings are compatible with the model (5) and the value for $\xi$.

### B. NaOH solution

In Fig. 5 we plot the Soret coefficient of PS beads of different size in NaOH solution between 40° and 55° C. In this range $S_T$ varies little with temperature. The curves are calculated from Eq. (3) with $\zeta = -38$ mV and constant values for $S_{\rm NaOH}$ and $\alpha_{\rm NaOH}$, as given in Table I. The data for beads of 90, 136, and 215 nm diameter follow roughly the linear size dependence of Eq. (3); the slight discrepancy might be related to the surfactant-free surface, and thus slightly higher $\zeta$-potential, of the homemade 90 and 136 nm sample, in contrast with the commercial 215 nm beads.

As a corollary, we note that our discussion of the data of Figs. 4 and 5 implies that solutions of NaCl and NaOH strongly differ in their thermal diffusion behavior. The strong temperature dependence of Fig. 4 is related to the variation of the coefficients in Eq. (5), which are qualitatively confirmed by experiment [40, 41]. The data of Fig. 5 suggest that $S_{\rm NaOH}$ and $\alpha_{\rm NaOH}$ do not depend on $T$; we are not aware of an experimental study on this point.

The coefficients $S$ and $\alpha$ result from the heat of trans-

port $Q_{\pm}$, which in turn are given by the ionic solvation enthalpy [39, 43]. Besides the electrostatic self-energy, these latter quantities comprise van der Waals and hydration contributions which are not easily evaluated. In the view of the well-known specific ion effects, as expressed for example in the Hofmeister series for protein solutions [44], it would not come as a surprise that NaCl and NaOH strongly differ in their solvation enthalpies.

## VI. DISCUSSION

Together with Eq. (3) the data presented in the above figures show that the Soret effect of PS beads originates essentially from thermal diffusion of the salt and the electrolyte Seebeck effect, thus confirming previous works [11, 13]. As a most important novel finding, our data show moreover that the Seebeck effect and diffusiophoresis in the salt gradient lead to the strong temperature dependence in NaCl solution. Although the variation with $T$ is similar to the behavior observed for various ionic and non-ionic colloidal suspensions [26], our measurements give clear evidence that there are two distinct mechanisms at work: Whereas a study on lysozyme protein shows that the temperature dependence of the Soret data results from a non-ionic interaction [22], the present work indicates that charge effects are dominant for polystyrene beads.

So far all experimental studies reported an increase with temperature, which is generally well fitted by the Piazza's phenomenological law $S_T = S_T^{\infty}(1 - e^{(T^*-T)/T_0})$ that changes sign at $T = T^*$; extrapolating our NaCl data gives $T^* \approx 15°$ C which roughly agrees with the values of [23, 26]. On the other hand, the data in NaOH solution presented in Fig. 5 provide the first example for a $T$-independent Soret coefficient. This finding enforces our above statement that the Soret motion of PS beads is a charge effect and thus has a strikingly different temperature dependence.

There remains the question why the non-ionic mechanism at work in protein and micellar solutions and the charge mechanism of latex particles in NaCl solution, show such a similar temperature dependence. Piazza and coworkers pointed out that the non-ionic interaction is strongly correlated with the thermal expansivity $\beta$ of water [26]. On the other hand, a similar correlation is known to occur between the thermal diffusion factor $\alpha_{\mathrm{NaCl}}$ of sodium chloride and $\beta$ [40]. The data of Fig. 4 suggest that there is a similar relation between the electrolyte Seebeck coefficient $S_{\mathrm{NaCl}}$ and the expansivity of water. In this picture, the thermal expansion of water would be at the origin of the temperature dependence of Soret data for non-ionic polymer solutions, proteins, and charged PS particles. By contrast, the data of Fig. 5 indicate a very different behavior of NaOH solution. The physical origin of such ion-specific effects [18, 19] could be related to the Hofmeister effect observed for protein solutions.

**Acknowledgment.** A.W. acknowledges support through the Leibniz program of Universität Leipzig during the summer term 2013, and thanks the groups of Frank Cichos and Klaus Kroy for their kind hospitality.


[1] S. Wiegand, *J. Phys. Cond. Matt.*, 2004, **16**, 357.
[2] J.K. Platten, *J. Appl. Mech.*, 2006, **73**, 5.
[3] R. Piazza, *Soft Matter*, 2008, **4**, 1740.
[4] A. Würger, *Rep. Prog. Phys.*, 2010, **73**, 126601.
[5] S. Duhr, D. Braun, *Phys. Rev. Lett.* 97, 2006, 038103.
[6] H.-R. Jiang, H. Wada, N. Yoshinaga and M. Sano, *Phys. Rev. Lett.*, 2009, **102**, 208301.
[7] Y.T. Maeda, A. Buguin, A. Libchaber, *Phys. Rev. Lett.*, 2011, **107**, 038301.
[8] H.-R. Jiang, N. Yoshinaga, M. Sano, *Phys. Rev. Lett.*, 2010, **105**, 268302.
[9] I. Buttinoni, G. Volpe, F. Kümmel, G. Volpe, C. Bechinger, *J. Phys.: Condens. Matter*, 2012, **24**, 284129.
[10] B. Qian, D. Montiel, A. Bregulla, F. Cichos, H. Yang, *Chem. Sci.*, 2013, **4**, 1420.
[11] S.A. Putnam, D.G. Cahill., *Langmuir*, 2005, **21**, 5317.
[12] A. Würger, *Phys. Rev. Lett.*, 2008, **101**, 108302.
[13] D. Vigolo, S. Buzzaccaro and R. Piazza, *Langmuir*, 2010, **26**, 7792.
[14] A. Majee, A. Würger, *Phys. Rev. E: Stat., Nonlinear, Soft Matter Phys.*, 2011, **83**, 061403.
[15] Y. He, M. Tsutsui, R.H. Scheicher, F. Bai, M. Taniguchi, T. Kawai, *ACS Nano*, 2013, **7**, 538.
[16] A. Majee, A. Würger, *Phys. Rev. Lett.*, 2012, **108**, 118301.
[17] A. Majee, A. Würger, *Soft Matter*, 2013, **9**, 2145.
[18] K.A. Eslahian , M. Maskos, *Colloids Surf., A: Physicochem. Eng. Aspects*, 2012, **413**, 65.
[19] T. Lang , K.A. Eslahian , M. Maskos, *Macromol. Chem. Phys.*, 2012, **213**, 2353.
[20] R. Piazza, Guarino, *Phys. Rev. Lett.*, 2002, **88**, 208302.
[21] S. Fayolle, T. Bickel, S. Le Boiteux, A. Würger, *Phys. Rev. Lett.*, 2005, **95**, 208301.
[22] S. Iacopini, R. Piazza, *Europhys. Lett.*, 2003, **63**, 247.
[23] S.A. Putnam, D.G. Cahill, G.C.L. Wong, *Langmuir*, 2007 **23**, 9221.
[24] S. Wongsuwarn, D. Vigolo, R. Cerbino, A.M. Howe, A. Vailati, R. Piazza, P. Cicuta, *Soft Matter*, 2012, **8**, 5857.
[25] A. Königer, N. Plack, W. Köhler, M. Siebenbürger, M. Ballauf, *Soft Matter*, 2013, **9**, 1418.
[26] S. Iacopini *et al.*, *Eur. Phys. J. E*, 2006, **19**, 59.
[27] H. Ning, S. Datta, T. Sottmann, S. Wiegand, *J. Phys. Chem. B*, 2008, **112**, 10927
[28] M. Martin, C. van Batten, M. Hoyos, *Thermal Nonequilibrium Phenomena* in *Fluid Mixtures*. ed. W. Köhler, S. Wiegand, Lecture Notes in Physics 584; Springer: Berlin, Heidelberg, 2002
[29] M.E. Schimpf, K. Caldwell, J.C.Giddings, J. C, *Field-flow fractionation handbook*, Wiley-Interscience: New York, NY, 2000

[30] J.E. Belgaied, M. Hoyos, M. Martin, *Journal of Chromatography A* 1994, **678**, 85
[31] J.J. Gunderson, K.D. Caldwell, J.C. Giddings, *Separation Science and Technology* 1984, **19**, 667
[32] M.S.-D. Juang, I.M. Krieger, *J. Polym. Sci. Polym. Chem. Ed.* 1976, **14**, 2089
[33] M. Braibanti, D. Vigolo, R. Piazza, Phys. Rev. Lett. **100**, 108303 (2008).
[34] S. Fayolle, T. Bickel, A. Würger, *Phys. Rev. E: Stat., Nonlinear, Soft Matter Phys.*, 2008, **77**, 041404.
[35] E. Ruckenstein, *J. Coll. Interf. Sci.*, 1981, **83**, 77.
[36] J.L. Anderson, *Annu. Rev. Fluid Mech.*, 1989, **21**, 61.
[37] K.-R. Huang, J.-S. Chang, S. Chao, K.-C. Wu, C.-K. Yang, C.-Y. Lai, S.-H. Chen, *J. Appl. Phys.*, 2008, **104**, 064702.
[38] K. I. Morozov, *J. Exp. Theo. Phys.*, 1999, **88**, 944.
[39] J.N. Agar *et al.*, *J. Phys. Chem.*, 1989, **93**, 2079.
[40] D.R. Caldwell, *J. Phys. Chem.*, 1973, **77**, 2004.
[41] F.S. Gaeta *et al.*, *J. Phys. Chem.*, 1982, **26**, 2967.
[42] M. Antonietti, L. Vorwerg, *Colloid Polym Sci*, 1997, **275**, 883.
[43] A. Würger, *Comptes Rendus Ac. Sci. Méc.*, 2013, **341**, 438
[44] Y. Zhang, P.S Cremer, *Current Opinion in Chemical Biology* 2006, **10**, 658